BULLETIN OF THE POLISH ACADEMY OF SCIENCES
TECHNICAL SCIENCES, Vol. 66, No. 3, 2018
DOI: 10.24425/123444

Pulse powered turbine engine concept – numerical analysis of influence of different valve timing concepts on thermodynamic performance

P. TARNAWSKI* and W. OSTAPSKI

Institute of Machine Design Fundamentals, Warsaw University of Technology, 84 Narbutta St., 02-524 Warsaw, Poland

Abstract. The present work is an attempt to create the concept of an engine that will combine the benefits of a pulse powered piston engine and continuously powered turbine engine. The paper focuses on the subject of pressure gain combustion (PGC). A turbine engine concept with stationary constant volume combustors, working according the Humphrey cycle, is presented. Its work has to be controlled by valve timing system. Four different valve timing concepts were analyzed. Their influence on thermodynamic performance of engine was evaluated. Different valve constructions were researched by means of 3D numerical computational fluid dynamics (CFD) simulation.

Key words: pressure gain combustion (PGC), constant volume combustion (CVC), turbine engine, CFD analysis, valve timing.

1. Introduction

Internal combustion engines utilized as power supply can be divided into the continuous powered and the pulse powered. A classical turbine engine is powered continuously, while a piston engine is an example of a pulse powered unit. Apart from different conversion of mechanical work, the process of combustion is also fundamentally different. In the continuously powered engine combustion is isobaric, whereas in a pulse powered one combustion can be isobaric, isochoric-isobaric or isochoric.

From the thermodynamic point of view, isochoric combustion is more efficient than isobaric combustion. During isochoric combustion pressure growth can be obtained. Thus further expansion is realized from the higher pressure level, which has a beneficial effect on overall engine efficiency. During isobaric combustion pressure is constant, thus expansion is realized from the pressure level obtained in a compressor.

The second issue that is of relevance here concerns different cooling rates. High constant temperature in a combustion chamber of turbine engine requires a substantial air cooling rate, i.e. high excess of compressed air $\lambda = 3.3–6$ [1]. Thus high compressor power is required. In turn, maximum temperature in the pulse powered piston engine appears for a relatively short period of time as compared to the entire combustion time. Moreover, during filling cold, compressed air cools down the hot walls of the combustion chamber. Piston engines are cooled mostly by liquid. As a result, a pulse powered engine requires a relatively smaller amount of power to compress air (excess air is in the range of $\lambda = 0.85–1.65$ [2]). This is a big advantage over a continuously powered one, with beneficial influence on overall engine efficiency.

A continuously powered turbine engine has significant advantage over a pulse powered piston engine regarding the ratio of engine power to engine mass. In the case of aviation, this is an important aspect which contributes to reducing fuel consumption. For example, the Rolls-Royce M250-C20B turbine engine has an indicator of the power-to-mass ratio of 4.3 kW/kg, whereas the M67D44 diesel piston engine produced by BMW has it at 1.26 kW/kg [3].

This work is an attempt to create the concept of an engine that will combine the benefits of pulse powered and continuously powered engines. Incorporation of constant volume combustion would contribute to increasing engine efficiency. Application of a turbine would decrease the engine weight. The engine would then find its use in helicopters [4].

Presented in the paper pulse powered turbine engine concept is powered by energy pulses, entirely different than a classical, continuously powered turbine engines. The engine works according to Humphrey's thermodynamic cycle. Its analitycal evaluation is carried out in section 2. The engine work requires realization consecutive stages of: preparation of high-pressure gases in combustion chambers and supplying the turbine with these gases. An operation of engine according to the Humphrey cycle requires the use of the valve timing system.

In section 3, a 3D turbine engine with stationary constant volume combustors is presented. Four different valve timing constructions are proposed and its thermodynamic performance is evaluated. Different constructions are realized and evaluated by means of the 3D computational fluid dynamic tool (CFD). All simulations were carried out using the ANSYS Fluent commercial code ANSYS Fluent [5].

The pressure gain combustion (PGC) concept, that would contribute to increasing engine efficiency, has gained atten-

*e-mail: piotr.tarnawski@simr.pw.edu.pl

Manuscript submitted 2017-01-27, revised 2017-04-10, 2017-04-28, 2017-05-22 and 2017-06-05, initially accepted for publication 2017-06-06, published in June 2018.

tion in recent years [6]. Many different types of pressure gain combustors have been proposed to date [7]. Three of the most common ones are: the pulse combustor [8], the pulse detonation engine and the wave rotor [9–12]. "As regards the pulse combustor, in the early 1900s, Holzwarth and Griepe proposed gas turbine designs with nearly constant-volume combustion. In the Holzwarth design [13], multiple combustors are used to create a high-pressure pulsing flow stream. This stream axially impacts the blades of a turbine wheel. The Griepe design [14] used multiple combustion chambers around the periphery of a radial inflow turbine, but acknowledged ineffective use of wave action in the combustion chamber. Other designs [15, 16] sought to improve thermal efficiency, but no practical gas turbine was commercialized with stationary constant-volume combustors. Challenges reported included inefficient flow process and work extraction from combustion gases, idle and part-load performance, low specific power, and cumbersome mechanical components" [7].

2. Comparison of Humphrey cycle with common thermodynamic cycles

A contemporary engine works according to different thermodynamic cycles and is thus characterized by different efficiencies. Four engine cycles were taken under consideration in the comparison. Those included: the Otto cycle, the Diesel cycle, the Brayton cycle and Humphrey Cycle. The aim was to evaluate their efficiency for similar working parameters. The following assumptions were made:

- Air compression ratio of 12:1,
- Maximum combustion temperature of 2500 K,
- Intake temperature of 283 K, intake pressure of 0.1 MPa,
- Ideal gas model,
- All thermodynamic processes were reversible.

2.1. Otto vs. Diesel cycle efficiency. A spark ignition piston engine works according to of the Otto cycle. It consists of two isochoric processes (combustion and exhaust) and two adiabatic processes, i.e. compression and expansion (see entropy-temperature chart in Fig. 1). Efficiency for the Otto cycle reached 51%. It was calculated using equation (1). The efficiency in that cycle depends only on the compression ratio.

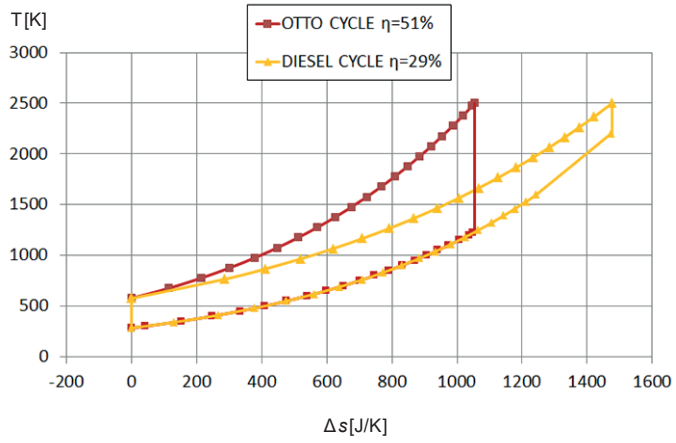

Fig. 1. Comparison of Otto and Diesel cycle efficiency

$$\eta_{OTTO} = 1 - \left(\frac{V_2}{V_1}\right)^{\kappa-1} \tag{1}$$

where: V_2 [m^3] – air volume after compression, V_1 [m^3] – air volume before compression, k – heat capacity ratio.

The auto ignition piston engine works according to the Diesel cycle. It consists of isobaric combustion, isochoric exhaust and two adiabatic processes, i.e. compression and expansion. Efficiency for the Diesel cycle reached 29% (see Fig. 1). It was calculated using equation (2). The efficiency depends on the compression ratio and engine load. Efficiency decreases with increasing load.

$$\eta_{DIESEL} = 1 - \frac{q_{out}}{q_{in}} = 1 - \frac{1}{\kappa}\frac{T_1}{T_2}\frac{\frac{T_4}{T_1} - 1}{\frac{T_3}{T_2} - 1} \tag{2}$$

where: q_{out} [J/kg] – exhausted heat, q_{in} [J/kg] – supplied heat, T_1 – intake temperature, T_2 – temperature after compression, T_3 – temperature after combustion, T_4 – temperature after expansion.

A optimum compression ratio in the Otto engine is 12–13 (3.3–3.6 MPa of compressed air). In reality however it is not possible to obtain this level because of emerging detonation combustion phenomena, which are dangerous for engine lifetime. In spark ignition piston engines real compression ratio is 6–10 (1.2–2.5 MPa of compressed air) [9].

The detonation combustion phenomena do not appear in the auto ignition piston engine. Thus a higher compression ratio can be used. If we assume using the Diesel cycle with a higher compression ratio but the same maximum temperature as in the Otto cycle, then the Diesel cycle will obtain higher efficiency. In reality, because of using a higher compression ratio, the auto ignition piston engine is generally more efficient than the spark ignition piston engine [9].

2.2. Brayton vs. Humphrey cycle efficiency. A classical turbine engine works according to the Brayton cycle. It consists of two isobaric processes (combustion and exhaust) and two adiabatic processes, i.e. compression and expansion. The efficiency of Bryton cycle was calculated from equation (3), reaching 50% (see Fig. 2). It depends only on the compression ratio.

$$\eta_{BRAYTON} = 1 - \left(\frac{p_1}{p_2}\right)^{\frac{\kappa-1}{\kappa}} \tag{3}$$

where: p_1 [Pa] – air pressure before compressor, p_2 [Pa] – pressure of compressed air.

A Humphrey cycle consists of isochoric combustion, isobaric exhaust and two adiabatic processes, i.e. compression and

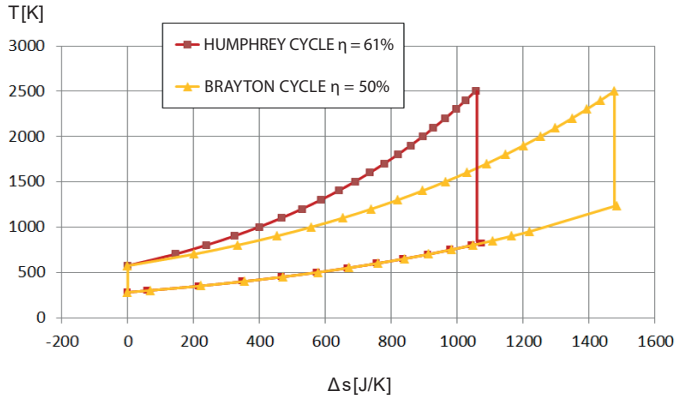

Fig. 2. Comparison of Brayton and Humphrey cycle efficiency

expansion (see Fig. 2). The cycle efficiency was calculated from equation (4), reaching the value of 61%. It is the highest among all four analyzed cycles and depends on the compression ratio and engine load. Efficiency increases with increasing load.

$$\eta_{HUMPHREY} = 1 - \frac{q_{out}}{q_{in}} = 1 - \frac{C_v(T_4 - T_1)}{C_p(T_3 - T_2)} \tag{4}$$

where: C_v – constant volume heat capacity, C_p – constant pressure heat capacity.

Turbine engines are generally less efficient than piston engines. For example, a modern GE marine turbine engine [19] with pressure ratio of 18:1 and power of 25 kW has 36% efficiency. Efficiency decreases with power, and for small units the value is below 30%. As regards engines working according to the Humphrey cycle, no practical gas turbine was commercialized to date [6].

The Humphrey cycle can be realized as an impulse powered turbine engine. Combustion should proceed in a constant volume combustion chamber. Then expansion has to be realized in de Laval nozzle where a gas accelerates to high velocity at the exit. The kinetic energy of gas should be transformed to mechanical work in turbine. As the process continuous, parameters in the combustion chamber change, as though in an emptying a pressure tank. Pressure and temperature decreases in the combustion chamber. It makes the whole process highly unsteady. The engine works in repeating series of cycles and has to be controlled by valves. As a result of valve rotation, filling and exhaust is realized. Four different types of valves are investigated in the next section.

3. Different valve timing concepts – CFD simulation study

3.1. Principle of operation of a pulse powered turbine engine. Pulse powering can be realized by means of valve timing. The roller valve, whose geometric model is presented in Fig. 3, was the first to be analyzed. It consisted of the supply valve, the

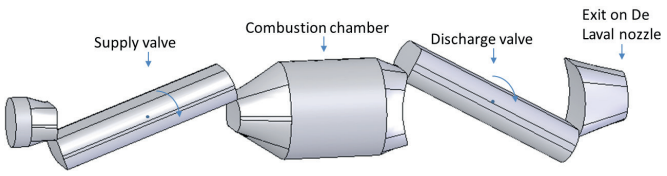

Fig. 3. Fluid model of valve timing with roller valves

discharge valve and a stationary combustion chamber. Both valves rotated at the same velocity of 350 rad/s (3342 rpm).

The valves were constructed to control the cycle of engine operation when they rotate at constant speed. One engine cycle consisted of the following stages:

- fresh air filling – duration: 0.002 s,
- combustion – duration: 0.0045 s (direct fuel injection: 0.002s plus afterburning: 0.0025 s),
- exhaust on turbine – duration: 0.003 s.

Duration of each stage was evaluated based on CFD simulations.

After opening of the supply valve, fresh, compressed air filled the combustion chamber. Next, when two valves were closed, injection of fuel took place and the combustion process started. At the end of cycle, the discharge valve opened and exhaust on the turbine began. After the exhaust stage, the engine cycle was repeated. Two cycles were realized during one valve rotation. See the valves arrangement during operation of the engine cycle in Fig. 4.

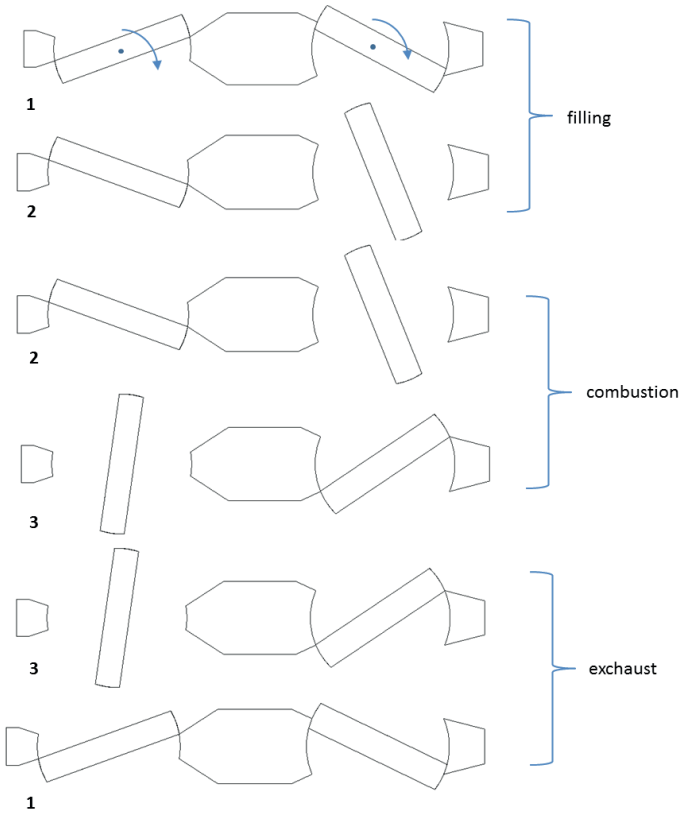

Fig. 4. Arrangement of valves during operation of engine cycle

3.2. Simulation of filling and combustion process. The operation of the supply system with roller valves was simulated. The geometry was discretized by hexahedron elements (see Fig. 5). The numerical model contained a species transport for a mixture of gases including CH_4, O_2, N_2, CO_2 and H_2O. A compressible semi-ideal model of gas was incorporated. Turbulence was modelled with a realizable k-e model. Rotating valves were modelled using dynamic mesh capability with prescribed rotation velocity using profiles. Pressure based, coupled, transient solver was set with time step of 0.00001 s [20].

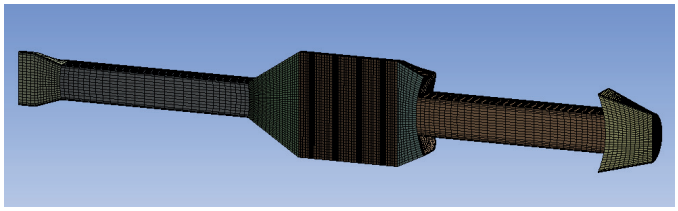

Fig. 5. Numerical mesh of valve timing with roller valves

After opening the supply valve, fresh, compressed air (with pressure of 1.2 MPa and temperature of 450 K) filled the combustion chamber. The air mixed with the rest of the combustion gases remaining in the chamber (see Fig. 6). This took 0.002s.

After filling, when two valves were closed, injection of fuel took place (see Fig. 7). The simulation was carried out assuming injection of methane gas. The Eddy dissipation model of combustion was used [20]. Based on the oxygen content after filling (19%) and the assumed air excess factor of 1.25, the amount

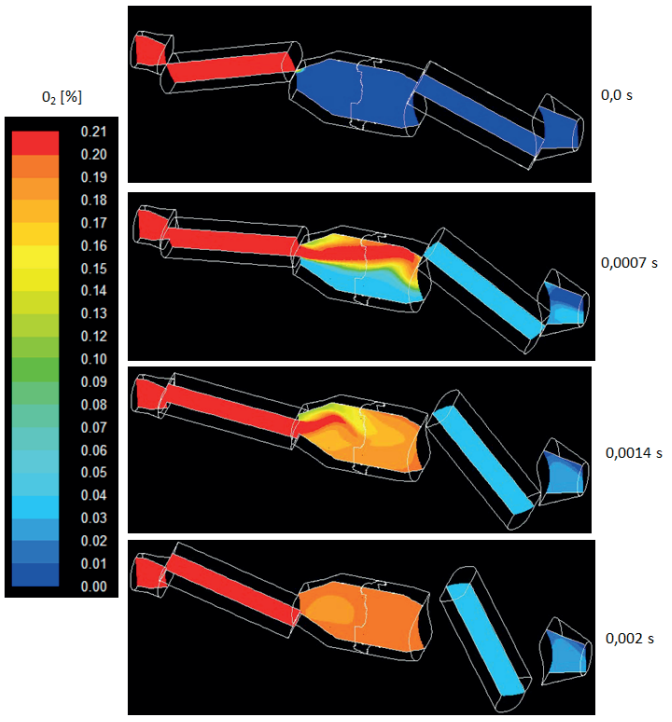

Fig. 6. Simulation of the filling stage – oxygen content

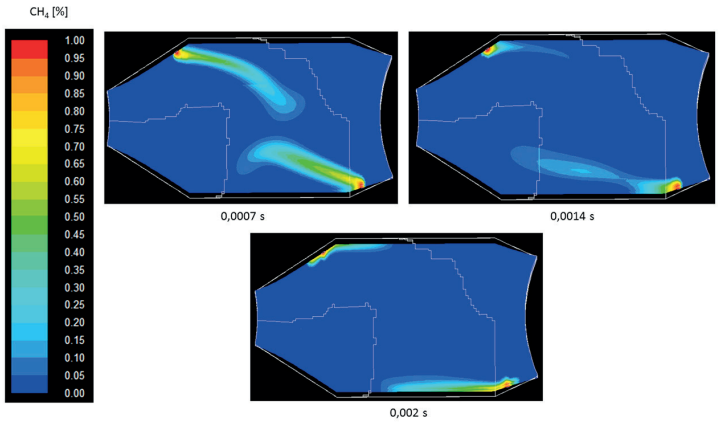

Fig. 7. Fuel injection simulation – methane content

of injected gas was calculated (0.0000705 kg). The specific combustion heat of methane was 50000 [MJ/kg]. The volume of combustor was 0.00025 m^3.

During combustion that lasted 0.0045 s, the pressure went up to 5.3 MPa (see Fig. 8). Maximum temperature reached 2482 K (21, 22, 23).

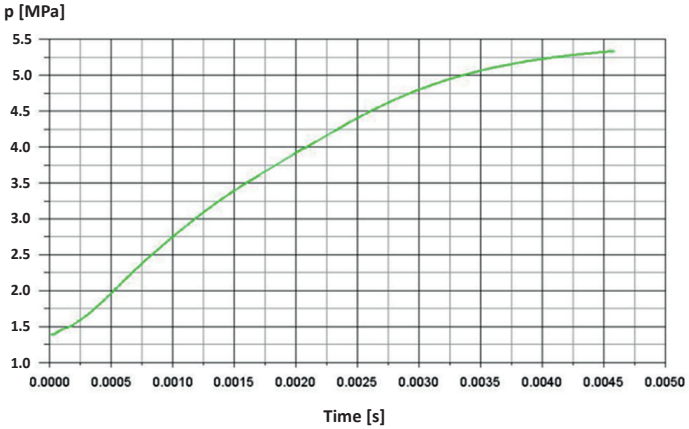

Fig. 8. Pressure growth during isochoric combustion

Combustion efficiency reached 97% as per (5).

$$\eta_{COMBUSTION} = \frac{E_{generated}}{E_{fuel}} \tag{5}$$

where: $E_{generated}$ [J] – energy generated during combustion, E_{fuel} [J] – injected chemical energy.

3.3. Exhaust with roller valve. After isochoric combustion, the exhaust valve opened to start the exhaust process. The expansion of combustion gases was realized in the de Laval nozzle with 2.5 ratio of outlet cross section area to critical cross section area. The critical cross section diameter was 26 mm. The nozzle was set at the angle of 82 degrees to turbine axis. The supersonic profile of the turbine blades had to be incorporated

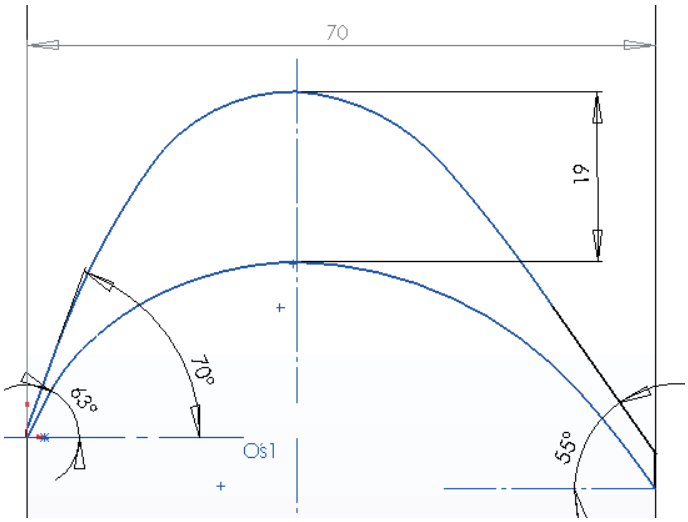

Fig. 9. Incorporated supersonic profile of turbine blades

(see the blade profile used in Fig. 9). The turbine consisted of one stage that rotated at 26000 rpm, using sliding mesh capabilities [20]. Several turbine velocities were tested. The velocity of 26000 rpm was selected based on the highest work done in one cycle. External diameter of the turbine was 440 mm, and the height of the blades was 55 mm.

The characteristic dimensions of the roller valve are presented in Fig. 10. The valves rotated at 3342 rpm.

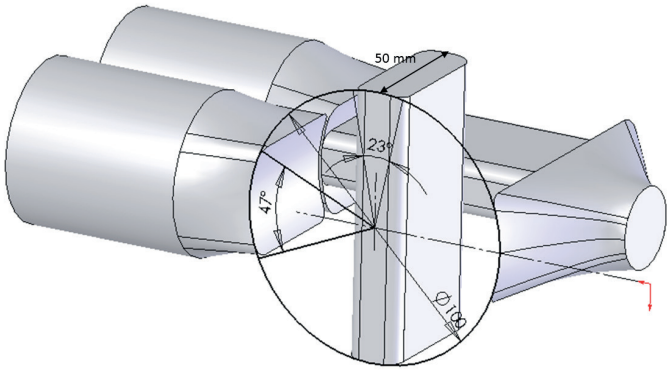

Fig. 10. Characteristic dimensions of the roller valve

On each expansion period (duration: 0.003 s), preparation of high-pressure gases is required (duration: 0.006 s). During pulse energy preparation, expansion does not appear. When expansion does not take place, aerodynamic resistance on turbine blades occurs, causing the negative moment. Thus two combustion chambers were used for just one nozzle. They were alternately expanded in a single de Laval nozzle. This was meant to reduce the idle period. The supply system was placed on both sides of the turbine diameter (see complete simulation model in Fig. 11 and its discretization in Fig. 12).

The engine cycle was repeated every 0.0045 s. The maximum moment reached 600 Nm. The moment averaged in

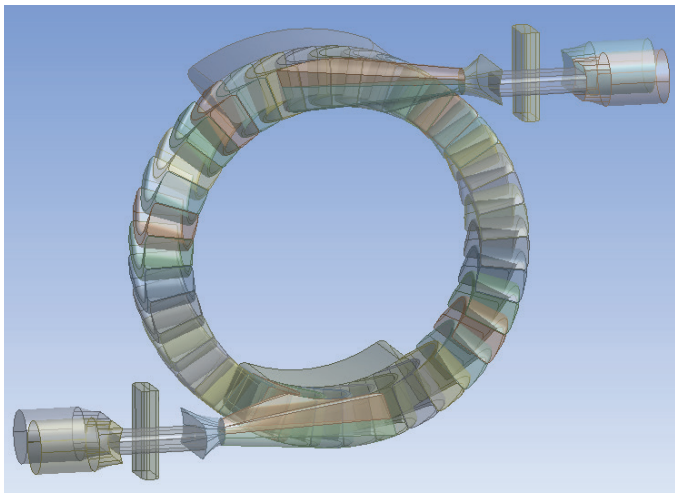

Fig. 11. Geometric model of an engine with roller valves

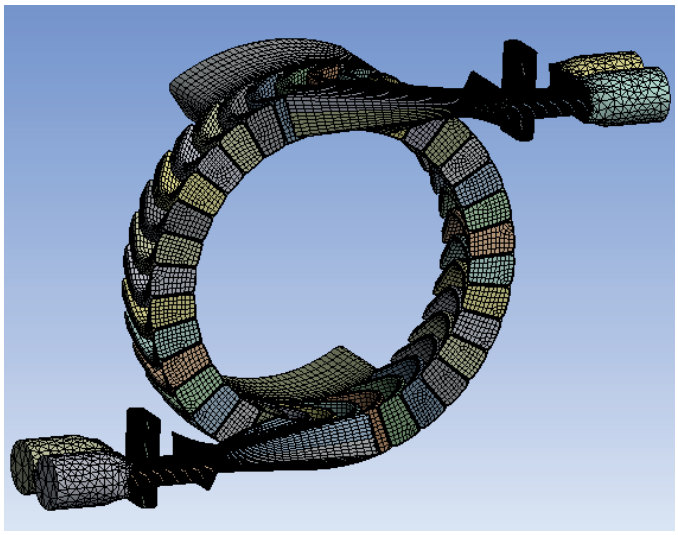

Fig. 12. Discretized model of an engine with roller valves

0.0045 s was 166.1 Nm (see Fig. 13). The value was arithmetically averaged based on data reported in each time step.

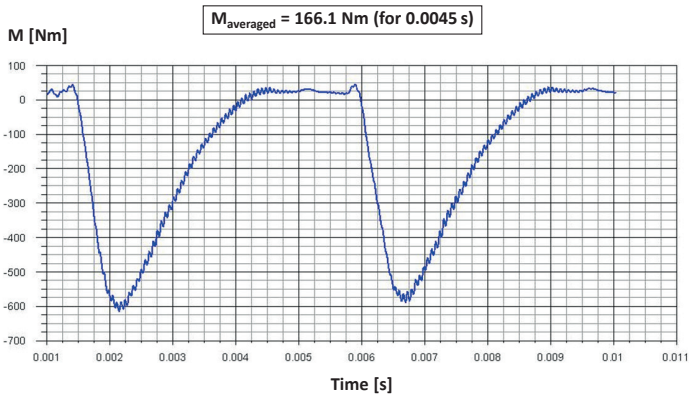

Fig. 13. Turbine moment for the roller valve case

Although two combustion chambers were used, unfavorable moment still appeared (idle period). It can be seen in Fig. 13, between 0.0045 and 0.006 s. This is because the preparation of high-pressure gas period was longer than expansion.

During expansion, the maximum Mach number reached 2.22 (see Fig. 14). This was in the highest peak moment.

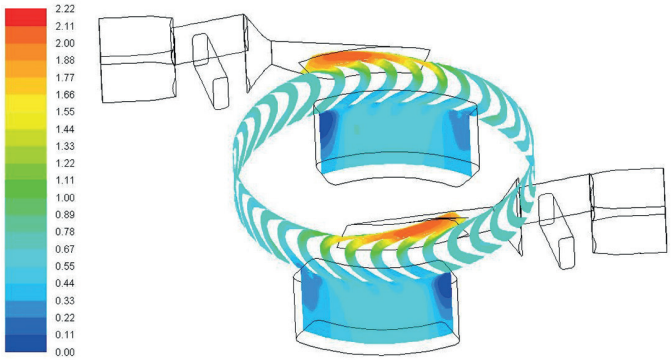

Fig. 14. Mach number distribution on turbine blades

Pressure distribution in the middle of turbine blades is presented in Fig. 15.

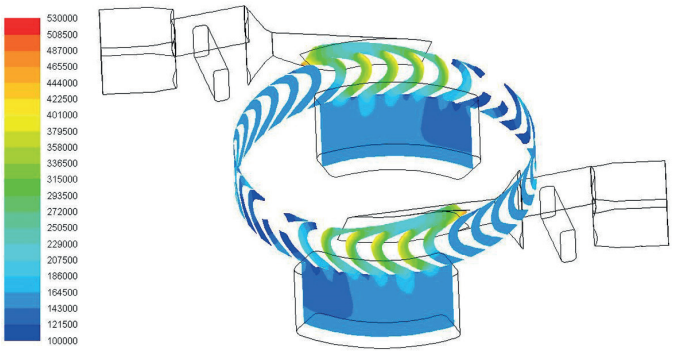

Fig. 15. Pressure distribution [Pa] on turbine blades

The work done by the turbine was equal 4.07 kJ (6).

$$L_{turbine} = \frac{M_{averaged} \cdot n \cdot t_{cycle}}{9549} \tag{6}$$

where: $M_{averaged}$ [Nm] – averaged moment, n [rpm] – turbine velocity rotation, t_{cycle} [s] – cycle time.

Engine efficiency reached 28.9% (6). The engine power obtained was 452.4 kW.

$$\eta_{ENGINE} = \frac{L_{turbine}}{E_{fuel}} \tag{7}$$

where: $L_{turbine}$ [J] – work obtained from the turbine, E_{fuel} [J] – injected chemical energy.

3.3. Exhaust with disc valve. The disc valve was the second to be analyzed (see Fig. 16). It was used with four combustion chambers. When in the two chambers combustion was realized, in the second two exhaust took place. The chambers were opened two at a time. The valve speed rotation was set at 241 rad/s (2392 rpm).

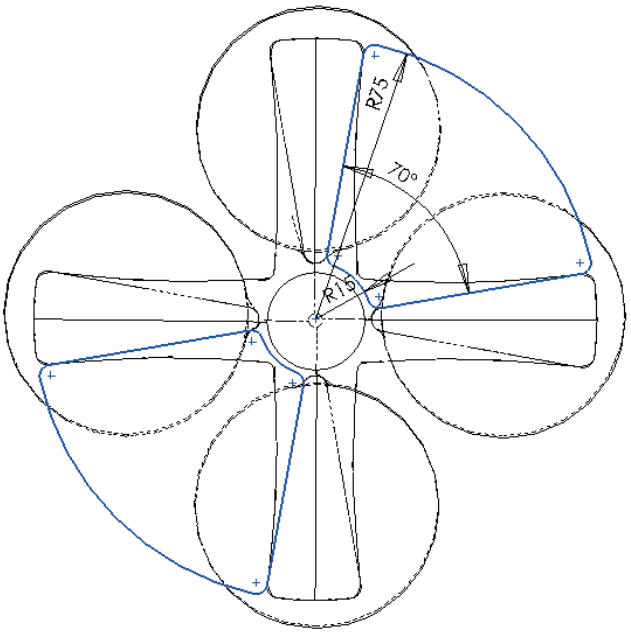

Fig. 16. Characteristic dimensions of the roller valve

The engine with a disc valve is shown in Fig. 17.

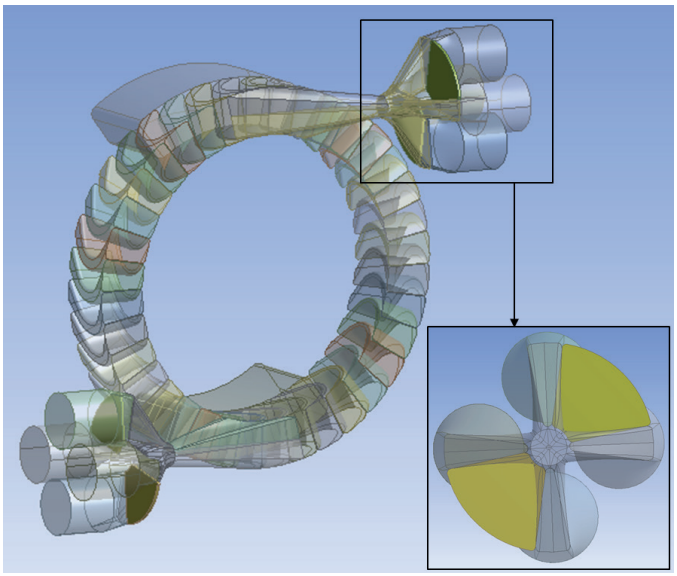

Fig. 17. Geometric model of an engine with disc valves

The one engine cycle was repeated every 0.0065 s. The maximum moment reached was 800 Nm. The moment averaged

in 0.0065 s was 247.6 Nm (see Fig. 18). In that case, turbine velocity was set at 30000 rpm. The higher turbine velocity set in that case provided more produced mechanical work. Total engine efficiency reached 35.8% and the power was 777.5 kW.

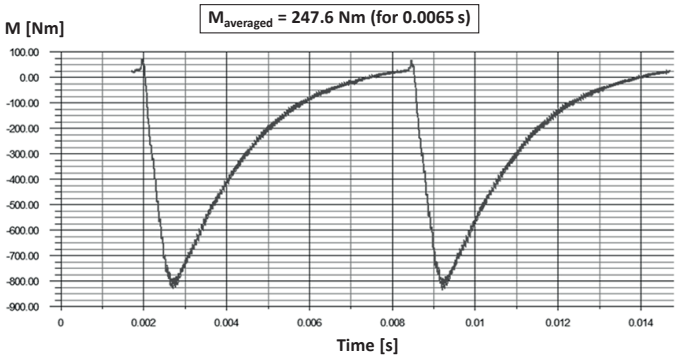

Fig. 18. Turbine moment for the disc valve case

Improvement of efficiency of about 6.9% was obtained. Implementation of the disc valve and four chambers allowed equating the combustion time and expansion time. It reduced the idle period almost to zero.

The valve speed rotation was decreased to 241 rad/s (2392 rpm). Despite this, the opening speed was higher, the reason being that the two chambers were opened two at a time.

3.4. Exhaust with disc valve and split nozzle. Some geometric changes were introduced along with the disc valve. The first concerned splitting the de Laval nozzle into two separate ones (see Fig. 19). Moreover, the height of the blades was reduced from 55 to 40 mm. This allowed for covering more blades (from 4 to 6 blades) by the nozzle exit with the same amount of combustion gases. The disc valve remained unchanged.

The average moment reached 258.4 Nm and efficiency stood at 37.5% (see Fig. 20). Efficiency increased by about 1.7% as compared with the model with only one nozzle.

Splitting of the nozzle allowed for better directing of gas onto blades. Moreover, more blades were working, reducing the losses caused by partial turbine load.

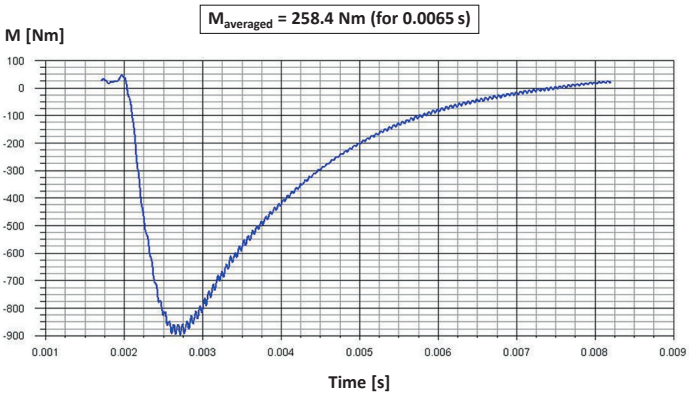

Fig. 20. Turbine moment for disc valves and split nozzle

3.5. Exhaust with disc valve supplying along the entire perimeter. An effort for the nozzles to cover the entire turbine perimeter was undertaken. The power of the engine had to be doubled as the engine consisted of 16 combustion chambers. The height of blades was decreased to 25 mm. The single outlet nozzle covered 4 blades (see Fig. 21).

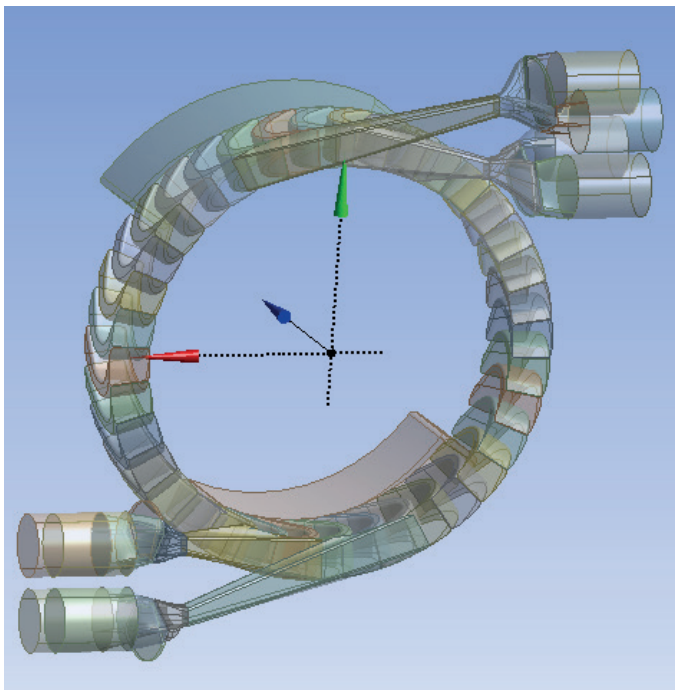

Fig. 19. Geometric model of an engine with disc valves and split nozzle

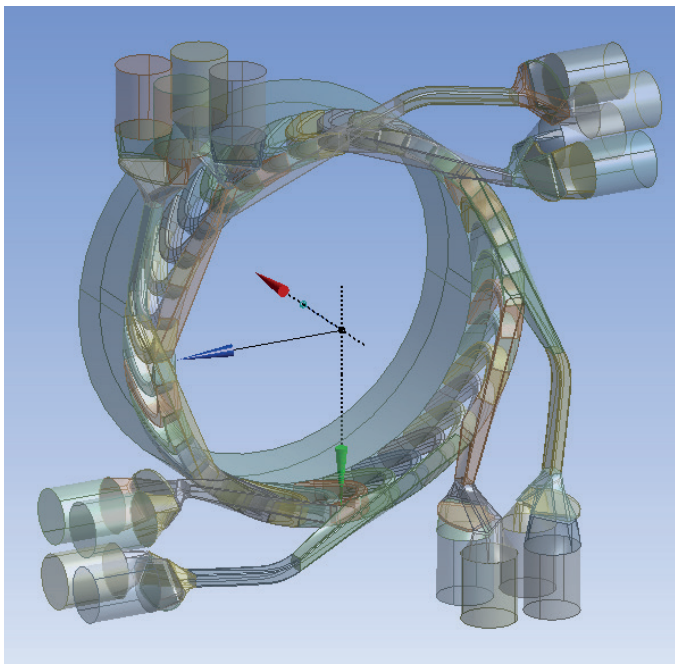

Fig. 21. Geometric model of an engine with disc valves, supplying the entire diameter

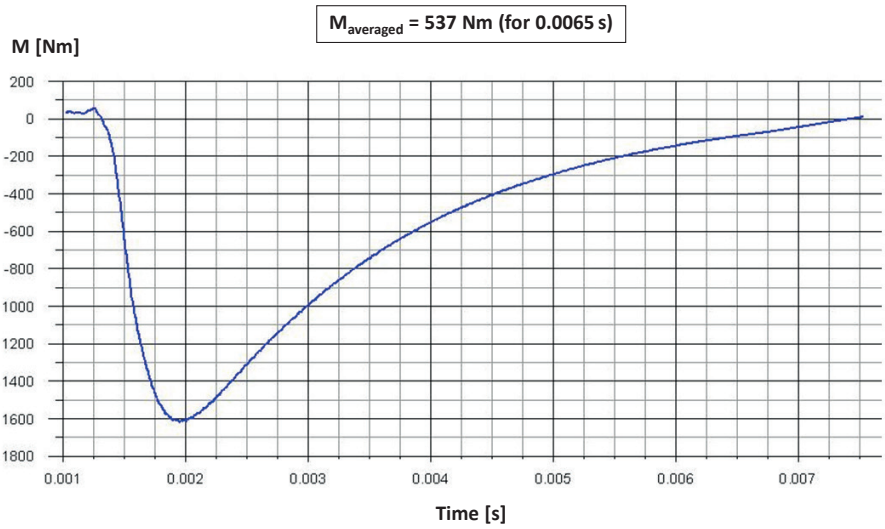

Fig. 22. Turbine moment for disc valves, supplying the entire diameter

The 537 Nm averaged moment was obtained (see Fig. 22). Total engine efficiency reached 39.0% and power was 1687 kW. Efficiency increased by about 1.5% as compared with the previous case.

Supplying on entire turbine perimeter effectively reduced losses caused by partial turbine loading. Realization of that construction required introduction of long supply channels, which could be problematic in practical realization (e.g. high heat losses).

3.6. Exhaust with middle valve. The middle valve was the third to be analyzed. It rotated in the middle of four combustion chambers that were placed circumferentially. It rotated at 241 rad/s, providing the same cycle as with the disc valve. The geometric model is presented in Fig. 23 and Fig. 24.

The averaged moment of 256.5 Nm was obtained (see Fig. 25). Turbine velocity was set at 30000 rpm. Total engine efficiency reached 37.2%. It is about 1.4% better than with the disk valve and single nozzle.

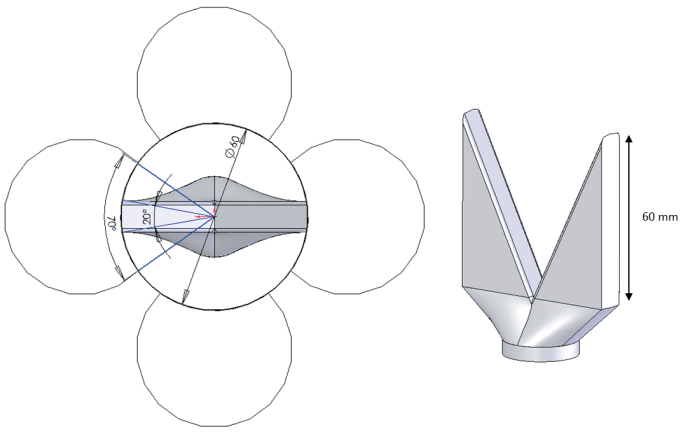

Fig. 23. Characteristic dimensions of the middle valve

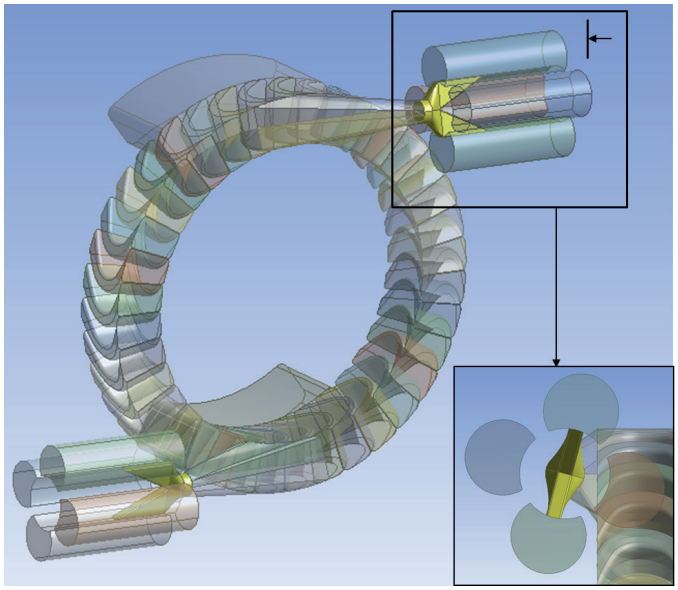

Fig. 24. Geometric model of an engine with middle valves

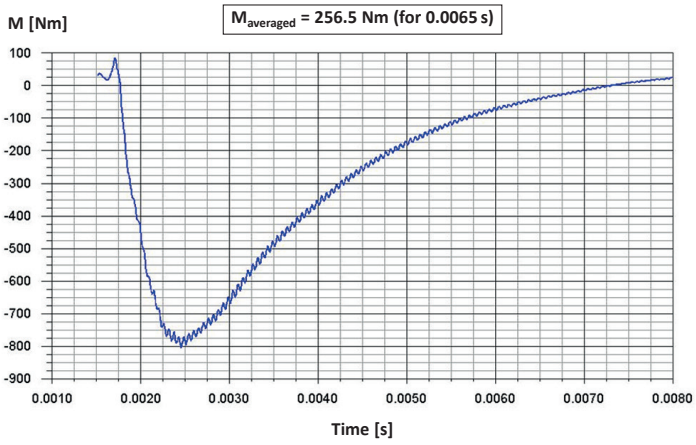

Fig. 25. Turbine moment for the middle valve case

The efficiency gain of 1.4% would be caused by twice smaller volume of the divergent part of the nozzle. During valve opening, the gas firstly fills the divergent part of the nozzle and then expand further. The smaller the divergent part of the nozzle, the smaller the losses suffered.

3.7. Exhaust with flap valve. The flap valve was the last to be analyzed. One valve was prescribed to one combustion chamber. It rotated at 241 rad/s, providing the same cycle time as for the dick valve. Moreover, the same chamber volume was used. The valves geometry is presented in Fig. 26 and Fig. 27.

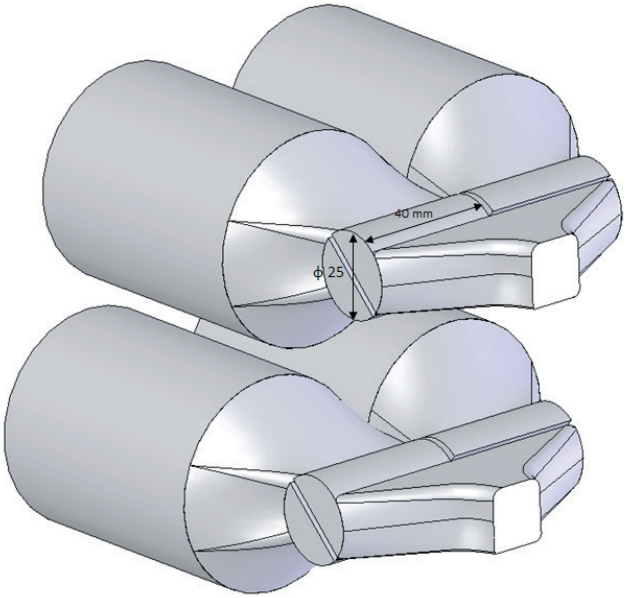

Fig. 26. Characteristic dimensions of the flap valve

The averaged moment of 254.5 Nm was obtained (see Fig. 28), with turbine velocity set to 30000 rpm. Total engine efficiency reached 36.9%. It was about 0.6% lower than with the dick valve.

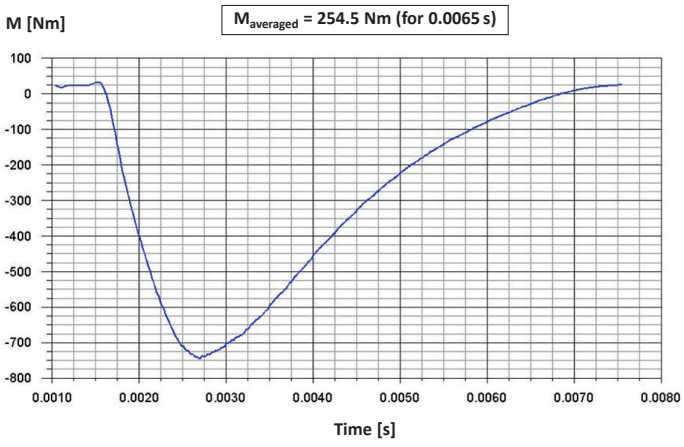

Fig. 28. Turbine moment for the flap valve case

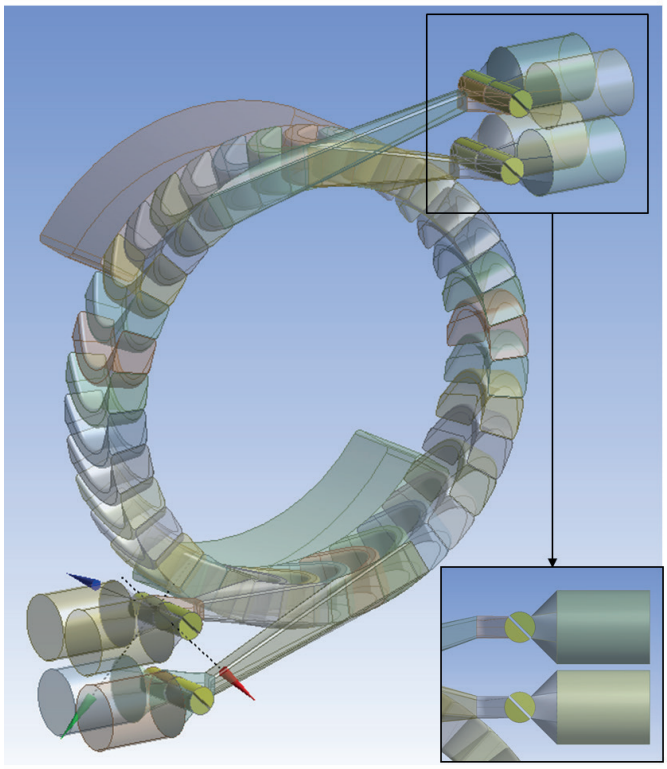

Fig. 27. Geometric model of an engine with flap valves

Slightly lower efficiency would be caused by slower opening of the valves. Even though rotation velocity of the valve was the same, the diameter of the valve was smaller. This accounts for it lower circumferential velocity.

4. Conclusions

Humphrey ideal cycle had the highest efficiency (61%) among all of the four cycles analyzed. It was about 10% better than the Otto cycle. This demonstrates the potential gain to be noted when realizing the engine with the Humphrey cycle.

The effort of realization of the Humphrey cycle with different valve timing constructions was presented. Four different valve timing constructions were proposed and their thermodynamic performance evaluated. Different constructions were realized and evaluated by means of 3D numerical simulation (CFD). Engine efficiencies for the following cases were obtained:

- the roller valve: 28.9%,
- the disc valve: 35.8%,
- the disc valve with a split nozzle: 37.5%,
- the disc valve supplying the entire diameter: 39%,
- the middle valve: 37.2%,
- the flap valve: 36.9%.

Incorporating of the disc valve and four chambers improved efficiency by about 6.9%, reaching the value of 35.8%. This allowed equating the combustion time and expansion time. It also reduced the idle period almost to zero. Moreover, opening

speed of the valves was higher. This was because two chambers were opened parallelly.

The losses caused by partial turbine loading were eliminated in the case of supplying the entire perimeter. The efficiency improvement was about 3.2%, reaching the value 39%.

Engine performance with the middle valve and flap valves was very similar to the disc valve. The engine efficiency difference for these cases was 1.4%.

Beside numerical analysis of the valves, a feasibility study of their real constructions would be of significance.

Generally, pulse powering is more difficult in realization than continuous powering. It is because the expansion process has to be intermitted. Losses are generated during valve opening and during the idle period.

Moreover, thermodynamic conditions during expansions (pressure, temperature, velocity) change with time, which causes problems with matching geometry to the current flow conditions. Namely, the expansion was realized in constant de Laval configuration of critical cross-section to outlet cross-section. Moreover, the de Laval nozzle was set at a constant angle to the turbine. All these factors contributed to lowering engine efficiency.

The highest efficiency obtained in the paper reached 39%. To compare it, Diesel and classical turbine engine examples are quoted. For example, the Diesel engine efficiency for helicopter uses evaluated according to [3] reached 44%. In turn, a gas turbine with continuous supply for helicopter application evaluated according to [24] reached 28% with the simple cycle and 34% with recuperation.

It is worth reminding here that heat losses caused by cooling and turbine velocity reduction by gears were not included in the present study. These two lower engine efficiency. If pulse powered engine performance was in the middle of the Diesel and classical turbine performance, the concept would be interesting. But the engine concept requires further research and improvements.

References

[1] Podręczny poradnik mechanika, Podstawowe informacje o turbinach gazowych, [in Polish]: http://www.softdis.pl/
[2] http://autowiedza.republika.pl/proces_spalania.html.
[3] M. Szlachetka, K. Pietrykowski, and P. Magryta, "Badania symulacyjne bilansu cieplnego silnika Diesla przeznaczonego do napędu lekkiego śmigłowca", *Logistyka* 6, (2014) [in Polish].
[4] W. Ostapski, T. Wierzchoń, J. Rudnicki, and S. Dowkontt, "Simulation and bench studies of the constructively and technologically modernized high performance piston aircraft engine", *Bull. Pol. Ac.: Tech.* 65 (1), (2017), doi: 10.1515/bpasts-2017–0012.
[5] ANSYS Fluent, www.ansys.com/Products/Fluids/ANSYS-Fluent.
[6] "New Developments in Combustion Technology Part II: Step change in efficiency", Princeton-CEFRC, 2012.
[7] "Review of recent developments in wave rotor combustion technology", *Journal of Propulsion and Power* 25 (4), 833–844 (2009). http://dx.doi.org/10.2514/1.34081
[8] J. Hwang, Y. Park, C. Bae, J. Lee, and S. Pyo, "Fuel temperature influence on spray and combustion characteristics in a constant volume combustion chamber", *Fuel* 160, 424–433, (2015), https://doi.org/10.1016/j.fuel.2015.08.004
[9] M. Razi Nalim, "A review of wave rotor and its applications", *J. Eng. Gas Turbines Power* 128(4), 717–735 (2006).
[10] J. Piechna, "Micro ring-engine numerical fluid dynamics analysis", *Archivum Combustionis* 34 (1), 1–26 (2014).
[11] K. Kurec, J. Piechna, and N. Müller, "Numerical investigation of the micro radial disk internal combustion engine", *Archivum Combustionis* 34 (1), 1–25, (2014).
[12] K. Kurec, J. Piechna, and K. Gumowski, "Investigations on unsteady flow within a stationary passage of a pressure wave exchanger, by means of PIV measurements and CFD calculations", *Applied Thermal Engineering* 112, 610–620, (2017), https://doi.org/10.1016/j.applthermaleng. 2016.10.142.
[13] H. Holzwarth and E. Junghans, "Improvements in Gas Turbines," U.K. Patent No. 20, 546, 1906.
[14] A. Griepe, "Gas Turbine-Engine," U.S. Patent No. 910, 665, 1909.
[15] H. Hagen, "Constant Volume Combustion Gas Turbine with Intermittent Flows," U.S. Patent No. 3, 877, 219, 1975.
[16] A. Gertz, "Gas Turbine Engine," U.S. Patent No. 4, 241, 576, 1980.
[17] J. Szargut, *Termodynamika Techniczna*, Wydawnictwo naukowe PWN, Warszawa 1991 [in Polish].
[18] "Gasoline could match diesel efficiency by 2025: increased investment will improve spark ignition's efficiency", *Automotive Engineer* 5(1), (2015).
[19] www.geaviation.com/marine/engines/commercial/25-mw-engine.
[20] ANSYS FLUENT User's Guide.
[21] K. Rajesh, J. Siddhant, V. Gaurav, and K. Avinash, "Laser ignition and flame kernel characterization of HCNG in a constant volume combustion chamber", *Fuel* 190, 318–327 (2017), doi.org/10.1016/j.fuel.2016.11.003.
[22] L. Labarrerea, T. Poinsot, A. Dauptaina, F. Duchainea, M. Bellenouec, and B. Boust, "Experimental and numerical study of cyclic variations in a constant volume combustion chamber", *Combustion and Flame* 172, 49–61 (2016).
[23] S.-W. Lee1, H.-S. Lee, Y.-J. Park, and Y.- S. Cho, "Combustion and emission characteristics of HCNG in a constant volume chamber", *International Journal of Hydrogen Energy* 37 (1), 682–690 (2012), https://doi.org/10.1016/j.ijhydene.2011.09.071.
[24] N. Barinyima, P. Pericles, and N. Theoklis, "Performance assessment of simple and modified cycle turboshaft gas turbin", *Propulsion and Power Research* 2 (2), 96–106 (2013), https://doi.org/10.1016/j.jppr.2013.04.00.